1-ethyl-3-methyl imidazolium acetate, hemicellulolytic enzymes and laccase-mediator system: Toward an integrated co-valorization of polysaccharides and lignin from Miscanthus

María Catalina Quesada-Salas, Marie E Vuillemin, Justine Dillies, Rebecca Dauwe, Loubna Firdaous, Muriel Bigan, Virginie Lambertyn, Dominique Cailleu, Arash Jamali, Renato Froidevaux, et al.

1-ethyl-3-methyl imidazolium acetate, hemicellulolytic enzymes and laccase-mediator system: toward an integrated co-valorization of polysaccharides and lignin from *Miscanthus*

María Catalina QUESADA-SALAS[1], Marie E. VUILLEMIN[1], Justine DILLIES[2], Rebecca DAUWE[3], Loubna FIRDAOUS[2], Muriel BIGAN[2], Virginie LAMBERTYN[1], Dominique CAILLEU[4], Arash JAMALI[5], Renato FROIDEVAUX[2], Eric HUSSON[1*], Catherine SARAZIN[1*]

[1]Unité de Génie Enzymatique et Cellulaire GEC, UMR 7025 CNRS, Université de Picardie Jules Verne, 33 rue Saint-Leu, 80039 Amiens Cedex, France

[2]UMRT BioEcoAgro UMR1158, Institut Charles Viollette, INRAe, équipe Biotransformation/Biocatalyse et Enzymes - Université de Lille, Bâtiment PolytechLille, Cité Scientifique, 59655 Villeneuve d'Ascq, France

[3]UMRT BioEcoAgro UMR1158, Université de Picardie Jules Verne, 33 rue Saint-Leu, 80039 Amiens Cedex, France

[4]Plate-forme analytique de l'Université de Picardie Jules Verne, UFR Sciences, rue Dallery / Passage du Sourire d'Avril - 80039 Amiens Cedex

[5]Plate-forme de microscopie électronique de l'Université de Picardie Jules Verne, UFR Sciences, 33 rue Saint-Leu - 80039 Amiens Cedex

*Co-corresponding authors: catherine.sarazin@u-picardie.fr and eric.husson@u-picardie.fr

Highlights

- Efficient enzymatic production of monomeric sugars from *Miscanthus*.
- Isolation of a lignin-enriched fraction with mainly β-O-4' interunit bonds.
- Solubilization of phenolic compounds in [Emim][OAc] during pretreatment.
- Enzymatic production of *p*-hydroxybenzaldehyde in recycled diluted [Emim] [OAc].

Abstract

The pretreatment of *Miscanthus x giganteus* with the ionic liquid 1-ethyl-3-methylimidazolium acetate ([Emim][OAc]), followed by enzymatic hydrolysis and oxidative depolymerization, resulted in the efficient production of monomeric sugars and selective production of phenolic intermediates. The liquid fractions containing monomeric sugars were obtained with high yields (>80%), while a solid fraction enriched with lignin (>50% $w.w^{-1}$) was isolated. The phenolic monomers released during [Emim][OAc]-pretreatment were identified and quantified by HPLC. A decrease in the content of vanillin, vanillic acid, and *p*-hydroxybenzaldehyde was observed during pretreatment, suggesting a selective solubilization of guaicyl and *p*-hydroxyphenyl units from the lignin polymer in [Emim][OAc]. The decrease in *p*-coumaric and ferulic acids content suggested a cleavage of lignin-carbohydrate complexes during pretreatment. Both pretreatment and enzymatic hydrolysis affected the content of ferulic acid ether and ester bonds. The NMR structural study (2D HSQC) of the isolated lignin showed the preservation of β-O-4' interunit bonds, while ^{31}P NMR

analysis revealed a high content of aliphatic hydroxyl groups. The oxidative depolymerization of the isolated lignin, catalyzed by the laccase mediator system in the presence of 5% $v.v^{-1}$ recycled [Emim][OAc] in buffer, mainly led to the production of free *p*-hydroxybenzaldehyde as a promising platform molecule. The mass balance of glucan, xylan and lignin from *Miscanthus* was validated throughout this strategy.

Graphical abstract

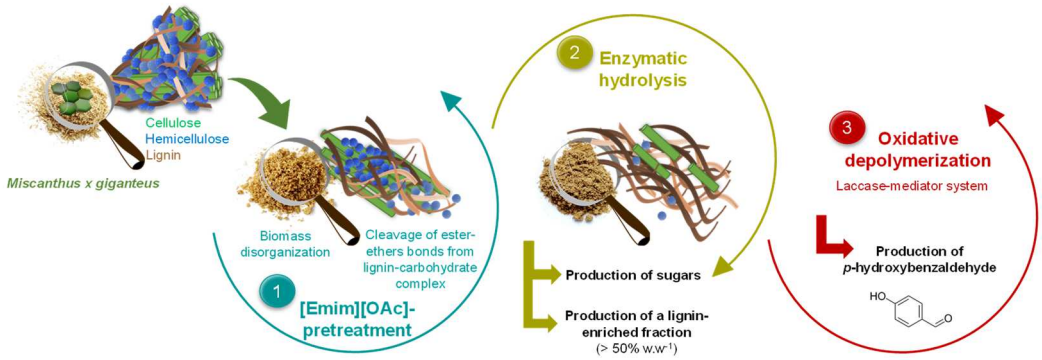

Keywords

Ionic liquid, pretreatment, enzymatic hydrolysis, enzymatic oxidative depolymerization, phenolic content, lignin structure.

1. Introduction

The co-valorization of the three main polymers obtained from lignocellulosic biomass (LCB) represents a key opportunity to ensure the economic viability and competitiveness of lignocellulosic biorefineries (Moreno et al., 2019; Narron et al., 2016). LCB polysaccharides, cellulose and hemicelluloses, have been

widely studied in terms of fractionation and conversion into platform molecules for the production of biofuels or chemicals, as an alternative to petroleum-based products (Bhatia et al., 2021; R. Bhatia et al., 2020; Klemm et al., 2005). Similarly, the lignin polymer constitutes the largest reservoir of aromatic compounds and has enormous potential as a renewable feedstock for the production of valuable phenolic intermediates (Sun et al., 2018; Wang et al., 2019; Zevallos Torres et al., 2020). Nonetheless, lignin is still considered as a by-product of the lignocellulosic biorefinery, with its applications currently restricted to low-value added products (2%) or cogeneration (Bajwa et al., 2019; Bertella and Luterbacher, 2020; Zhang and Naebe, 2021).

Various approaches, including mechanical, chemical, physico-chemical and biological, have been developed to fractionate LCB and make its polymers more accessible for further valorization (Baruah et al., 2018; Rezania et al., 2020). However, the process conditions of some of these approaches can generate uncontrolled modifications that affect the structural integrity of the polymers, especially for the lignin fraction. Furthermore, the complex and heterogeneous structure of lignin is highly sensitive to the extraction conditions of the most common lignin isolation processes (Kraft, lignosulfonate, soda, and Organosolv) (Bajwa et al., 2019; Kim and Um, 2020; Laurichesse and Avérous, 2014; Sethupathy et al., 2022). The use of inorganic salts, acids, strong bases, and organic solvents with questionable safety, are well known to greatly impact the chemical and structural properties of lignin (sulfur content and C-C bonds) and its reactivity, limiting the possibilities for chemical and enzymatic

transformations (Hulin et al., 2015; Patil et al., 2020; Talebi Amiri et al., 2019; Yu and Kim, 2020).

Ionic liquids (ILs) have been proven to be an excellent option to fractionate lignocellulosic biomass. While most studies have focused on improving the enzymatic digestibility of the polysaccharide fraction from pretreated biomass, new research interest has emerged in the recovery and valorization of the lignin fraction solubilized in ILs (Elgharbawy et al., 2016; Goshadrou and Lefsrud, 2017; Lee et al., 2022; Sathitsuksanoh et al., 2014; Smuga-Kogut et al., 2021; Usmani et al., 2020; Yoon et al., 2012). The recovery of lignin from ILs is not straightforward, often requiring the use of additional organic solvents or acidic reagents to induce precipitation (An et al., 2015; Brandt-Talbot et al., 2017; Ovejero-Pérez et al., 2020). Moreover, structural characterization of the recovered lignin revealed a decrease in the β-O-4' interunit linkages in the lignin polymer, suggesting a significant depolymerized and/or condensed state compared to milled wood lignin or cellulolytic enzyme lignin (Sathitsuksanoh et al., 2014; Sun and Xue, 2018; Tian et al., 2017).

Therefore, it seems relevant to focus on a lignin obtained from biomass pretreated with ionic liquid followed by enzymatic hydrolysis, which may preserve the structural integrity of this polymer. We may assume that the preserved structure would be more sensitive to depolymerization by oxidative enzymes while preserving the possibility of producing phenolic intermediates. To our knowledge, only a few studies have reported the transformation of this type of lignin into aromatic compounds. Particularly, Ninomiya and collaborators (Ninomiya et al., 2018) succeeded in a chemical oxidative depolymerization of

IL-enzymatic hydrolysis lignin, under drastic experimental conditions and the depolymerization profiles were compared to those of a soda lignin. A more sustainable alternative to convert the lignin polymer into phenolic intermediates is the oxidative depolymerization catalyzed by the laccase-mediator system (LMS, E.C. 1.10.3.2). However, the efficiency of laccase-catalyzed lignin depolymerization is limited by the very low solubility of the lignin polymer in aqueous enzymatic reaction medium (Harwardt et al., 2014; Singh Arora and Kumar Sharma, 2010) and the usual co-solvents or solvents (dimethyl sulfoxide, *N,N'*-dimethylformamide, acetone, dioxane) used to solubilize the lignin polymer are not suitable to maintain laccases structure and activity (Dillies et al., 2020). In this context, the present work reports the application of a sequential strategy on the dedicated crop *Miscanthus x giganteus* to co-valorize cellulose, hemicelluloses and lignin polymers. Short-time IL-pretreatment of *Miscanthus* at mild temperature was performed, followed by subsequent enzymatic hydrolyses catalyzed by (hemi)-cellulolytic enzymes, to generate monomeric sugars. Then, the isolated lignin-enriched solid fraction was subjected to enzymatic oxidative depolymerization to obtain high-value phenolic intermediates. The room temperature ionic liquid [Emim][OAc] was selected for its ability to dissolve LCB biopolymers and its acceptability in terms of eco-cytotoxicity and recyclability (S. K. Bhatia et al., 2020; Ostadjoo et al., 2018; Zhang et al., 2017). The impact of the steps performed on structural and chemical properties of the isolated lignin-enriched fraction was evaluated by biochemical, spectroscopic (FTIR, NMR), and microscopic (ESEM) methods providing additional chemical/structural details and mechanistic insights of phenolic compounds and the lignin polymer.

Finally, the feasibility of enzymatic oxidative depolymerization of the isolated lignin-enriched fraction catalyzed by a laccase-mediator system (LMS) was investigated for the first time in presence of the [Emim][OAc] used during the pretreatment step, as an alternative to the usual organic co-solvents. To confirm the validity of our approach, a mass balance of glucan, xylan and lignin was established.

2. Material and methods

2.1. Feedstock composition

Miscanthus x giganteus from organic farming in the *Hauts-de-France* region was provided by The *Institut Charles Viollette* (UMRT-BioEcoAgro UMR 1158, Lille, France). To ensure the homogeneity of the size of particles, *Miscanthus x giganteus* samples were milled with a planetary ball mill (Retsch MM400) during 90 s at a frequency of 25 s^{-1} to achieve a particle size of less than 800 μm (determined by SEM analysis). The biomass powder was freeze-dried (LABCONCO FreeZone 2.5, USA) to ensure a residual water content below 1% $w.w^{-1}$. The untreated and conditioned biomass of *Miscanthus x giganteus* is named as *Mxg* and its chemical composition (**Table *1***) was determined based on NREL protocols (Browning, 1967; Sluiter et al., 2012, 2005a, 2005b).

Table 1. Chemical composition of *Miscanthus x giganteus.*

Component		Experimental values (%w.w^{-1} DM)	Reported values for *Mxg* (%w.w^{-1} DM)
Ash		3.9 ± 0.1	3.1 ± 0.0[1]
Ethanol extractives		4.5 ± 0.6	6.7 ± 0.2[1]
Cellulose		46.2 ± 0.8	44.8 ± 0.2[2] // 50.34- 52.13[3]
Acid-insoluble lignin (AIL)		24 ± 1	22.8 ± 0.1[1] // 23.8 ± 2.7[4] // 24.1[5] (leaves) // 25.6[5] (stalks) // 18.86[6]
Acid-soluble lignin (ASL)		16 ± 2	0.9 ± 0.0[1] // 0.10[5] (leaves) // 0.11[5] (stalks)
Structural sugars	D-Glucose	45.2 ± 1.8	38.6 ± 0.2[1] (Glucan) // 45.3 ± 0.8[4] // 49.52[6]
	D-Xylose	21.7 ± 0.8	20.4 ± 0.1[1] (Xylan) // 22.13[6] // 22.3 ± 1.7[7]
	L-Arabinose	2.1 ± 0.1	2.8 ± 0.0[1] (Arabinan) // 3.26[6] // 3.4 ± 0.9[7]
	D-Galactose	0.7 ± 0.1	0.7 ± 0.0[1] (Galactan) // 0.62[6]

n=3, average values ± standard deviation. DM= Dry matter. Source: [1]R. Bhatia et al. (2020), [2]Auxenfans et al. (2014), [3]Brosse et al. (2012), [4] Auxenfans et al. (2017a), [5]Kim et al. (2012), [6]Le Ngoc Huyen et al. (2010), [7]Auxenfans et al. (2017b).

2.2. Chemicals and enzymes

1-ethyl-3-methylimidazolium acetate ([Emim][OAc], >98%,) was acquired from Solvionic S.A. (Verniolle, France). The enzymatic cocktail Cellic® Ctec 2 prepared at 15 FPU.g^{-1} of substrate (2.0 mg of glucose from 50 mg of filter paper has been designated as the intercept to calculate filter paper cellulase units (FPU) by IUPAC) and the laccase enzyme (specific activity ≥0.5 U.mg^{-1}; U: one unit corresponds to the amount of enzyme which converts 1 µmol of catechol per min at 25 °C and pH 5.0) from *Trametes versicolor* were supplied by Sigma-Aldrich (Steinheim, Germany). The ABTS, 2,2′-azino-bis(3-ethylbenzothiazoline-6-sulfonic acid) diammonium salt, was purchased from Roche Diagnostics (GmbH, Germany). D-glucose, D-xylose, L-arabinose, and

D-galactose were purchased from Sigma Aldrich (Steinheim, Germany), and D-cellobiose was purchased from MP Biomedicals (France). Vanillin, vanillic acid, vanillyl alcohol, 4-hydroxybenzoic acid, syringic acid, syringaldehyde, *p*-coumaric acid, ferulic acid, sinapic acid, benzoic acid, syringol, catechol, resorcinol, *p*-hydroxybenzaldehyde, 3,4,5-trimethoxycinnamic acid, *N*-hydroxypthalimide, chromium (III) acetylacetonate and 2-chloro-4,4,5,5-tetra-methyl-1,3,2-dioxaphospholane (TMDP), were provided by Sigma-Aldrich (Steinheim, Germany).

2.3. Co-valorization strategy for cellulose, hemicelluloses and lignin from *Mxg*

The general description of the implementation, based on [Emim][OAc]-pretreatment, enzymatic hydrolysis, and the laccase-mediator system is shown in **Figure 1**.

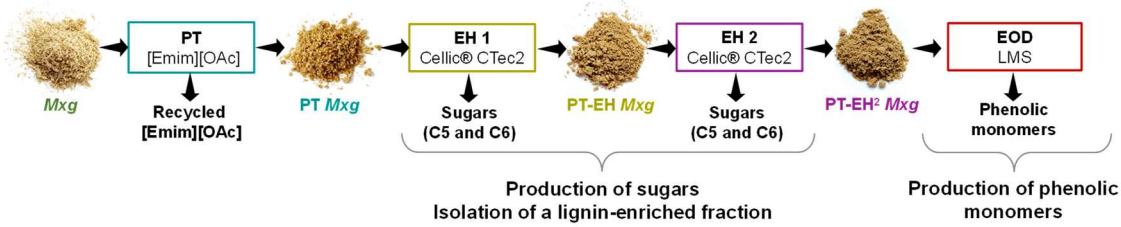

Figure 1. General co-valorization strategy of the three polymers of *Mxg*. *Mxg*= untreated *Miscanthus*. EH *Mxg*= hydrolyzed *Miscanthus*, PT *Mxg*= pretreated *Miscanthus*. PT-EH *Mxg*= pretreated and hydrolyzed *Miscanthus*. PT-EH^2 *Mxg*= pretreated and double hydrolyzed *Miscanthus*. PT= Ionic liquid pretreatment. EH= Enzymatic hydrolysis. EOD= Enzymatic oxidative depolymerization.

2.3.1. [Emim][OAc]-pretreatment

The pretreatment step (PT) was performed under the established conditions described by Auxenfans and collaborators (Auxenfans et al., 2014). Briefly, *Mxg* (2% w.v^{-1}) was added to [Emim][OAc] and incubated at 110 °C under vigorous

204 stirring for 40 min (n>3). The samples were cooled and ultrapure water (2:1
205 water: IL v:v) was added as antisolvent (vigorous stirring, 30 min). Samples
206 were then centrifugated (13776 rcf, 10 min, 4 °C, Eppendorf Centrifuge 5810 R,
207 Germany) and the liquid fraction was recovered and placed in a rotary
208 evaporator (Büchi Rotavapor R-200) to recover the recycled [Emim][OAc]. The
209 recovered solid was successively washed with ultrapure water until a
210 conductivity of σ< 5 µS, and then freeze-dried. The recovered solid fraction is
211 named as pretreated *Miscanthus* (PT *Mxg*) (**Figure 1**).
212
213 2.3.2. Enzymatic hydrolysis
214 Enzymatic hydrolysis (EH) was performed following the conditions described by
215 Araya and collaborators. (Araya-Farias et al., 2019). Briefly, biomass (2% $w.v^{-1}$)
216 was added to citrate-phosphate buffer (50 mM, pH 5.5) with a final Cellic®
217 Ctec2 concentration of 15 $FPU.g^{-1}$ of substrate (n>3). Samples were incubated
218 at 50 °C for 72 h under continuous stirring (time to reach the maximum sugars
219 yield. Table A1. Supplementary data). The reaction was stopped by incubating
220 the samples at 90 °C for 20 min. Then they were centrifuged (13776 rcf, 10 min,
221 4 °C, Eppendorf Centrifuge 5810 R, Germany), the hydrolysis supernatant was
222 collected for the quantification of total sugars and the recovered solid was
223 consecutively washed with ultrapure water and freeze-dried. The recovered
224 solid fraction after enzymatic hydrolysis of *Mxg* is named hydrolyzed
225 *Miscanthus* (EH *Mxg*) and from PT *Mxg* is called pretreated and hydrolyzed
226 *Miscanthus* (PT-EH *Mxg*). A second hydrolysis was performed under the same

conditions with PT-EH *Mxg* as substrate producing the PT-EH^2 *Mxg* solid fraction (**Figure 1**).

2.3.3. Enzymatic oxidative depolymerization

Enzymatic oxidative depolymerization (EOD) was carried out in presence of the laccase from *Trametes versicolor* and ABTS (2,2′-azino-bis (3-ethylbenzothiazoline-6-sulfonic acid) diammonium salt as mediator (Laccase-Mediator System, LMS), under conditions adapted from the literature (Dillies et al., 2020; Harwardt et al., 2014). Twenty mg of PT-EH^2 *Mxg* (0.2% w.v^{-1}) were added to 250 μL of acetate buffer (0.1 M; pH 4.5), pure [Emim][OAc] or recycled [Emim][OAc], and kept at 30 °C for 24 h under continuous stirring. Then, ABTS and laccase solutions in acetate buffer (pH 4.5) were added to achieve a final reaction volume of 5 mL and a concentration of 0.5 g.L^{-1} and 20 U.mL^{-1}, respectively. Samples were maintained at 30 °C for additional 24 h. After the enzymatic reaction, the mixture was freeze-dried (LABCONCO FreeZone 2.5, USA), the recovered solid was dissolved in 1 mL of water: methanol (1:1) and kept in constant agitation at 25 °C for 24 h. The samples were centrifuged (11357 rcf, 10 min, *MiniSpin®* Eppendorf, Germany) and the supernatant was collected and stored at -20 °C until further HPLC analysis was performed for the identification and quantification of phenolic compounds.

2.4. Chemical composition

Total lignin (acid-insoluble lignin and acid-soluble lignin) and total structural carbohydrates of solid fractions were determined by two-step acid hydrolysis

(H_2SO_4 at 72% and 2.5%, n=3) according to the NREL Laboratory Analytical procedure (Sluiter et al., 2012). The content of phenolic monomers of solid fractions was determined following a basic hydrolysis (NaOH 4.0 M at 170 ° for 2 h and NaOH 2.0 M at 35 °C for 2 h) based on previous study (Auxenfans et al., 2017a). Phenolic monomers from basic hydrolysis supernatant or oxidative depolymerization supernatant were identified and quantified by high performance liquid chromatography (HPLC) equipped with a Symmetry C18 column (4.6 mmx250 mm) and a Waters photodiode array UV detector at 280 nm. The detailed procedures are presented in section 1. Material and methods. Supplementary data.

2.5. Analytical procedures

The solid fractions were characterized by infrared spectroscopy using a Shimadzu FT-IR 8400S spectrometer (Shimadzu, France) in the Attenuated Total Reflectance (ATR) analysis mode.

The lignin-enriched fraction (PT-EH^2 *Mxg*) was analyzed by NMR (nuclear magnetic resonance) after solubilization in dimethyl sulfoxide-d_6 (10% w.v^{-1}) using 1D and 2D NMR techniques. The experiments were performed on a spectrometer (Bruker Avance 600 MHz) equipped with a 5mm BBI probe operating at 150.9128 MHz (^{13}C channel) and 600.1700 MHz (^{1}H channel) at 25 °C. The HSQC cross signals were assigned based on the literature (Table A2. Supplementary data). A semiquantitative analysis of the HSQC cross-signal intensities in the aromatic region (δ_C/ δ_H 100-150/5.0-9.0) was performed according to the literature (Tarasov et al., 2018).

The quantification of hydroxyls groups of PT-EH[2] *Mxg* fraction was performed by ^{31}P NMR (Argyropoulos, 1995, 1994; Husson et al., 2019). NMR spectra were acquired using a 500 MHz spectrometer (Avance III HD 500 MHz, Bruker, 500,0800 MHz for ^{1}H canal) equipped with a 5mm BBI probe operating at 202,4360 MHz. The assignment was carried out according to the data in the literature and the functional OH group was calculated in relative amount (Argyropoulos et al., 2021; Crestini and Argyropoulos, 1997; Fi et al., 2013; Husson et al., 2019).

The morphology of the solid fractions was characterized using a Quanta 200 FEG Environmental Scanning Electron Microscope (ESEM, FEI Company, USA). The detailed procedures are presented in section 1. Material and methods. Supplementary data.

The error bars shown in the figures represent the standard deviation of the mean values. An analysis of variance (ANOVA) was performed followed by Tukey's test for multiple comparisons with a significance level of probability ($p < 0.05$) (JMP software).

3. Results and discussion

3.1. Sugar production and isolation of a lignin-enriched solid fraction

The content of glucan, xylan, monomeric sugars and lignin of the solid fractions was determined (**Figure 2**). The solid fraction recovered after [Emim][OAc]-pretreatment (PT *Mxg*) had a similar content of xylan and ASL compared to *Mxg*, whereas a significant increase in the glucan fraction and a significant reduction in the content of AIL were observed (**Figure 2.a**). The delignification

299 level correlated with the amount of solubilized lignin in [Emim][OAc] ionic liquid,
300 estimated at 10 ± 1 g.100 g^{-1} DM of *Mxg*. This capacity of [Emim][OAc] to
301 dissolve the lignin polymer from the lignocellulosic matrix may be related to its
302 ability to promote H-bonding, associated to its high Kamlet-Taft Basicity (β)
303 value of 0.95 (Lopes et al., 2017; Usmani et al., 2020). The PT *Mxg* fraction had
304 a higher D-glucose content than *Mxg,* while the content of D-xylose, L-
305 arabinose and D-galactose remained constant (**Figure 2.b**). Thereby, the
306 pretreatment with [Emim][OAc] did not significantly affect the carbohydrate
307 content which is advantageous over other pretreatments such as Organosolv,
308 liquid hot water or dilute acid- or alkali pretreatments. This could be of particular
309 interest to preserve LCB polymers for further transformation and not only for
310 bioethanol production (Husson et al., 2018).
311 The enzymatic hydrolysis of PT *Mxg* provided a solid fraction namely PT-EH
312 *Mxg* with a reduced content of glucan and xylan of 29 ± 1 and 8.1 ± 0.8 g.100
313 g^{-1} DM, respectively (**Figure 2.a**). Therefore, 82% of D-glucose and 92% of D-
314 xylose were recovered in the liquid fraction (supernatant), showing a substantial
315 improvement in the enzymatic digestibility of *Mxg* after pretreatment (<10% for
316 untreated *Mxg*) (Table A1. Supplementary data). The recovery of monomeric
317 sugars by effective polysaccharide hydrolysis led to lignin enrichment. The first
318 solid fraction enriched in lignin, PT-EH *Mxg,* had an AIL content of 43 g.100 g^{-1}
319 DM (**Figure 2.a**). Although high sugar yields were obtained during the first
320 enzymatic hydrolysis, the polysaccharide content of PT-EH *Mxg* remained
321 significant. Additional enzymatic hydrolysis of PT-EH *Mxg* further reduced the
322 glucan content (17 ± 1 g.100 g^{-1} DM) while no changes in xylan content were

observed. This allowed the isolation of a new solid fraction, caused by the removal of the glucan fraction, named PT-EH^2 *Mxg*, with an AIL content of 52 g of lignin.100 g^{-1} DM (**Figure 2.a**).

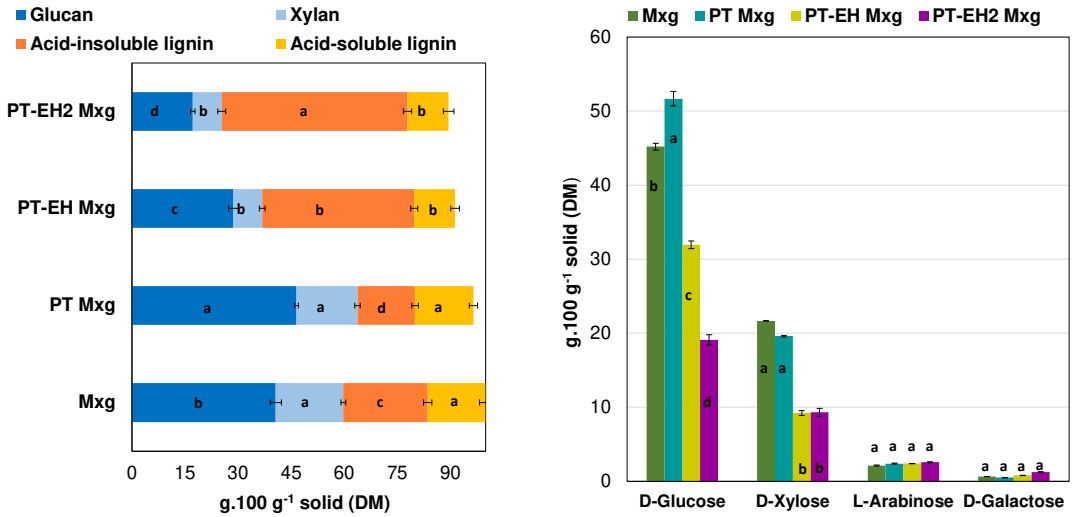

(a) **(b)**

Figure 2. Polysaccharide and lignin composition **(a)**, and sugar composition **(b)** of the recovered solid fractions after [Emim][OAc]-pretreatment and enzymatic hydrolyses of *Mxg*. Average values ± standard deviation. Different letters for the same component are significantly different ($p<0.05$).

3.2. Insight into the fate of phenolic compounds

The fate of guaiacyl (G) (*e.g* vanillin, vanillic acid, vanillyl alcohol), syringyl (S) (*e.g* syringic acid and syringaldehyde) and *p*-hydroxyphenyl (H) (*e.g* 4-hydroxybenzoic acid and 4 -hydroxybenzaldehyde) type monomers of the lignin polymer and identified in raw *Mxg*, was studied for each generated solid fraction (**Figure 3.a**). [Emim][OAc]-pretreatment significantly decreased the content of vanillin, vanillin acid, and *p*-hydroxybenzaldehyde by 54%, 27%, and 85%, respectively. The molar *S/G* ratio increased from 0.59 for *Mxg* to 0.90 for PT *Mxg*, suggesting a preferential removal of some G units during pretreatment. After enzymatic hydrolysis, the relative content of all phenolic compounds

increased slightly in PT-EH *Mxg* and PT-EH^2 *Mxg* compared to PT *Mxg* (**Figure 3.a**), illustrating the lignin enrichment in both fractions. The ratio *S/G* of PT-EH *Mxg* (0.90) and PT-EH^2 *Mxg* fractions (0.92) remained constant, suggesting a preservation of the structural units of the lignin polymer during enzymatic hydrolyses. For the final fraction enriched in lignin (PT-EH^2 *Mxg*) a S/G/H ratio of 40/44/16 was determined, which is consistent with the reported values for untreated *Miscanthus* (Jung et al., 2020).

Concerning the fate of hydroxycinnamic acids (ferulic and *p*-coumaric acids), *p*-coumaric acid content in raw *Mxg* was 18.8 mg.g^{-1}, mainly linked by ester-bonds (85%) (**Figure 3.b**). Ferulic acid was identified with a lower content of 4.6 mg.g^{-1} (**Figure 3.c**), while ester-linked to carbohydrates (65%) and ether-linked to lignin (35%). The pretreatment significantly decreased the content of both acids and modified the proportion of ether and ester bonds only for ferulic acid (**Figure 3.b** and **Figure 3.a**). Indeed, [Emim][OAc] induced cleavage of ferulic acid-lignin ether linkages significantly reducing ether bonds to 6%, while increasing ester bonds to 94%. On the contrary, both ester and ether bonds of *p*-coumaric acid decreased, probably due to cleavage of lignin-carbohydrates complexes (LCC) (Sathitsuksanoh et al., 2014; Yoo et al., 2017). After the first enzymatic hydrolysis, the content of ferulic acid in the PT-EH *Mxg* fraction was significantly reduced to 1.65 mg.g^{-1} confirmed by the release observed in the hydrolysate (data not shown). Ferulic acid content was then unchanged in PT-EH^2 *Mxg* fraction (**Figure 3.c**). However, the proportion of ether and ester bonds in ferulic acid was modified during enzymatic hydrolysis, returning to the same percentages as those observed in raw *Mxg* (**Figure 3.c**). Unlike ferulic

acid, enzymatic hydrolyses induced a significant increase in *p*-coumaric content to 20.4 mg. g^{-1} for the PT-EH[2] *Mxg* fraction, reaching the initial content observed in *Mxg* (**Figure 3.b**).

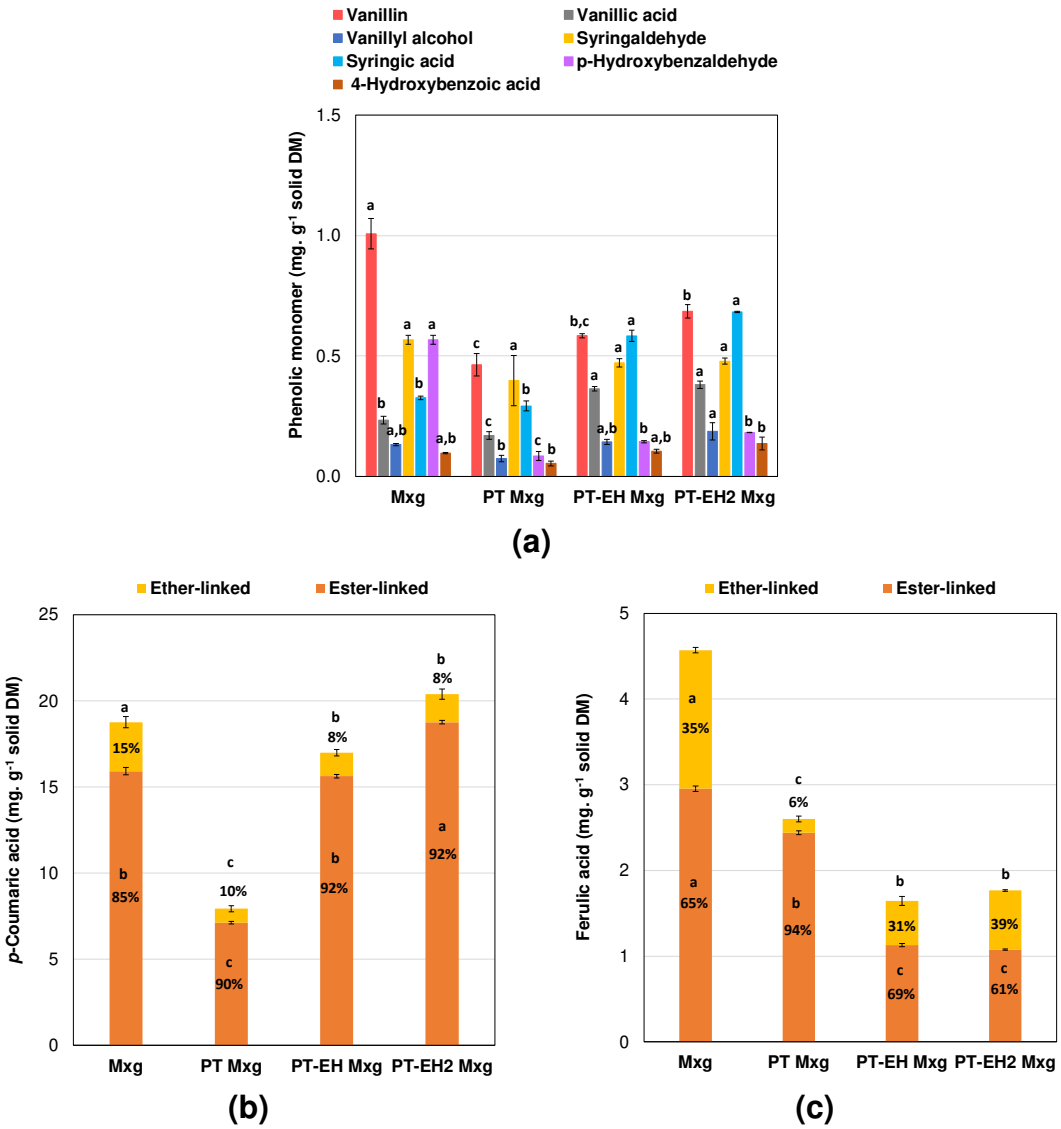

Figure 3. Phenolic monomers content **(a)**, ether- and ester-linked *p*-coumaric **(b)** and ether- and ester-linked ferulic acid **(c)** content of the recovered solid fractions before and after [Emim][OAc]-pretreatment and enzymatic hydrolyses of *Mxg*. Average values ± standard deviation. Different letters for the same phenolic compound are significant different ($p<0.05$). Different letters for the same type of bond (ether or ester) are significantly different ($p<0.05$).

3.3. Insight into the structure of the constitutive polymers

FTIR spectra of each generated solid fraction revealed the presence of polysaccharides and lignin in agreement with the results of chemical composition (**Figure 4)**. The band at 1156 cm^{-1} was attributed to the C1-O-C4' asymmetric stretching of cellulose and hemicelluloses and was more intense in *Mxg* and PT *Mxg* than in PT-EH *Mxg* and PT-EH^2 *Mxg* fractions, confirming the efficient enzymatic hydrolysis of polysaccharides.

The region between 1600 cm^{-1} and 1226 cm^{-1} reflected the contribution of the lignin polymer (Beckham et al., 2016; Horikawa et al., 2019; Wang et al., 2012). These characteristic bands of lignin (Table A3. Supplementary data) became more defined in the PT-EH *Mxg* and PT-EH^2 *Mxg* spectra (**Figure 4**) confirming the lignin enrichment. The determination of the cross-linked lignin (CLL) parameter (**Figure 4**) for each solid fraction suggested that a slight lignin condensation would occur throughout the processing steps. The structural changes observed by FTIR spectroscopy were confirmed by solid CP-MAS ^{13}C NMR, with observed modifications of polysaccharide fractions and lignin enrichment in the final solid fraction (PT-EH^2 *Mxg*) (Figure A2. Supplementary data).

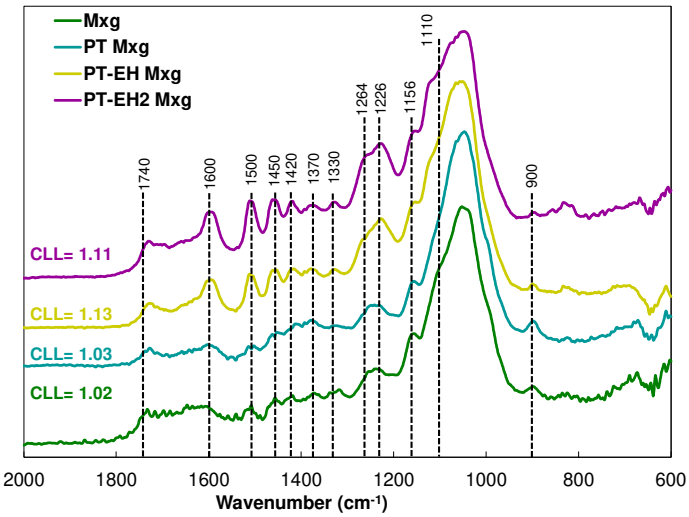

Figure 4. FTIR spectra of the recovered solid fractions before and after [Emim][OAc]-pretreatment and enzymatic hydrolyses of *Mxg.* CLL= Cross-linked lignin (Calculated as the ratio between band intensities at 1508 cm^{-1} and 1600 cm^{-1}).

Two-dimensional ^{1}H-^{13}C NMR was performed to provide essential information about the structural units and interunit linkages of the lignin polymer in the lignin-enriched fraction (PT-EH^{2} *Mxg*). Cross-signal assignment was performed according to literature data (Guo et al., 2020; Imman et al., 2021; Villaverde et al., 2009; Wang et al., 2018, 2012; Yuan et al., 2011; Zhao et al., 2017). The spectra of the side-chain (δ_C/ δ_H 50-100/ 2.0-6.0 ppm) and aromatic (δ_C/ δ_H 100-150/5.0-9.0) lignin regions are shown in **Figure 5**. The methoxy substituents (MeO) in the side chain region of the spectrum (**Figure 5.a**) were detected with a very prominent signal. The presence of carbohydrates (CHO) in the lignin-enriched fraction is confirmed by cross-signals in the δ_C/ δ_H 70-80/ 3-4 ppm region. Side chain signals from β-aryl-ether (β-O-4') interunit linkages were dominant (A_γ, A'_γ, A_α, $A_{\beta(G)}$ and $A_{\beta(S)}$), while cross-peaks corresponding to the linkages of the phenylcoumaran (β-5') and resinol (β-β') condensed substructures were not detected. The predominance of β-O-4' interunit linkages

in PT-EH^2 *Mxg* suggested a preservation of the lignin polymer structure after [Emim][OAc]-pretreatment and enzymatic hydrolyses of *Mxg*. This predominance has already been reported for a milled wood lignin from *Miscanthus x giganteus* (β-O-4'/ β-5'/ β-β'; 93/3/4), typically called "native lignin" (Villaverde et al., 2009).

Furthermore, in the aromatic region of the HSQC spectra (**Figure 5.b**), cross-signals from syringyl (S) and guaiacyl (G) lignin units were detected with high intensity. The presence of *p*-coumarate (*p*Ca) and ferulate (FA) substructures was well distinguished in the aromatic region, characteristic of herbaceous lignin. The S/G/H ratio was evaluated as 47/53/0 confirming the predominance of S- and G-units in the isolated lignin, similar value of a milled wood lignin from *Miscanthus* (44/52/4) (Hage et al., 2009).The S/G ratio of 0.90 obtained by HSQC agreed with the value determined from the phenolic monomer composition data (**Figure 3.a**). These results suggested the isolation of a lignin-enriched fraction with a preserved structure (high content of β-O-4' bonds) and few recondensed structures, in contrast to some technical lignins (Deuss and Kugge, 2021; Tian et al., 2017). These characteristics would be suitable to consider further efficient enzymatic oxidative depolymerization (Guo et al., 2020; Tian et al., 2017).

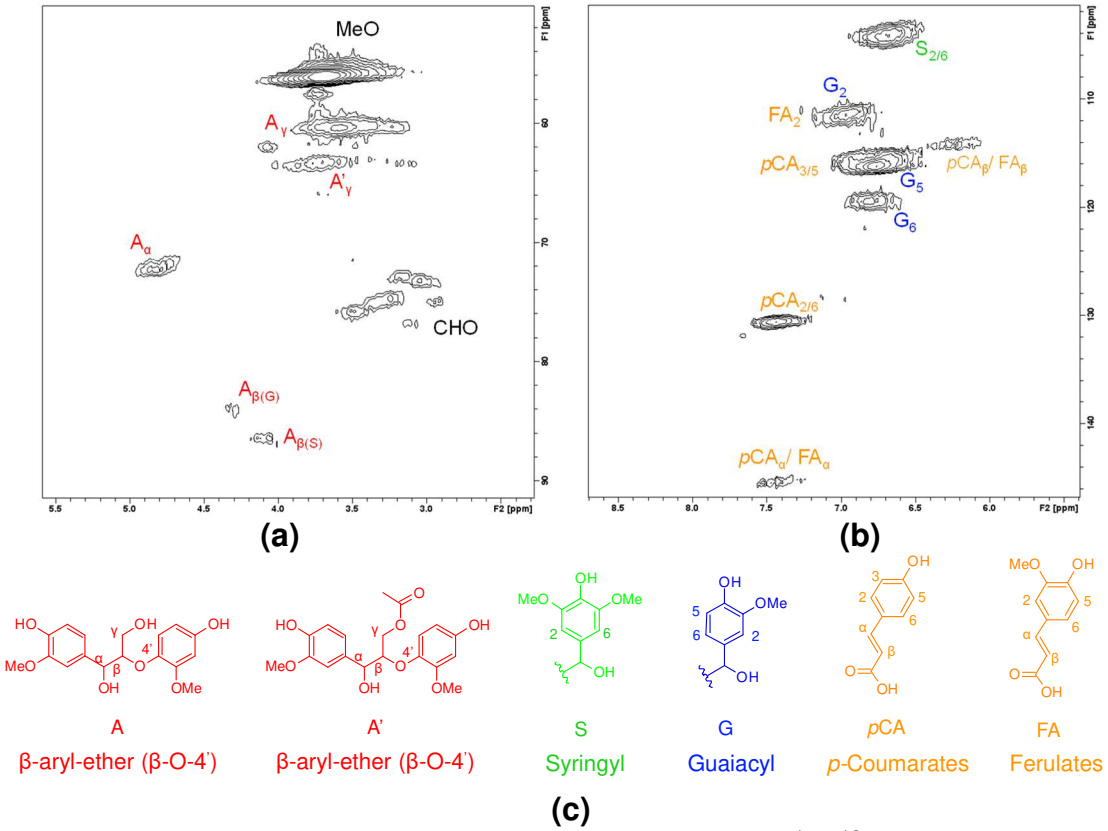

Figure 5.Side-chain **(a)** and aromatic **(b)** regions of the ^{1}H-^{13}C HSQC NMR spectra of the lignin-enriched fraction (PT-EH^{2} *Mxg*) and **(c)** main interunit linkages, units and substructures identified from the lignin polymer.

The ^{31}P -NMR spectra of PT-EH^{2} *Mxg* (**Figure 6**) obtained after derivatization is similar to the obtained for a “native lignin” from *Miscanthus x giganteus* (Hage et al., 2009), for which considerable amount of aliphatic hydroxyls groups and low amount of syringyl units were identified. The lignin-enriched fraction presented high relative content of aliphatic OH (~0.91) and lower content of OH-Syringyl (~0.006), OH-guaicyl (~0.03), OH-*p*-hydroxyphenyl (~0.03), and OH-carboxylic acid functional groups (~0.02) (**Table 2**). The signal attributed to OH-*p*-hydroxyphenyl may be principally the one of *p*-coumaric units, as previously described for an isolated lignin from *Miscanthus* (Hage et al., 2009) and also in agreement with the HSQC results.

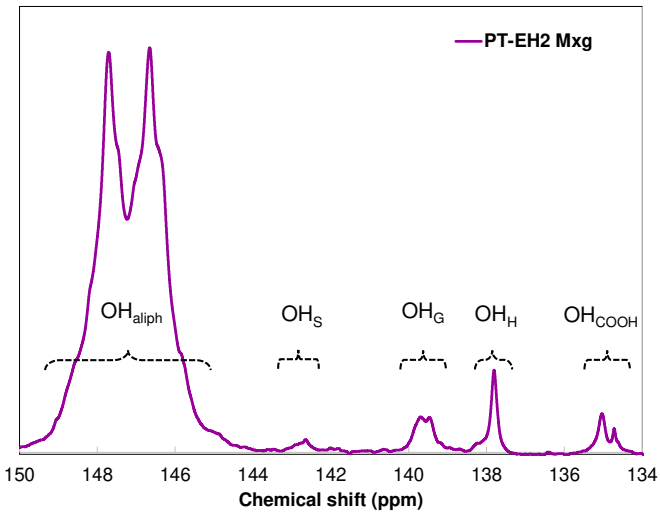

Figure 6. ^{31}P-NMR spectrum of PT-EH^2 *Mxg* after derivatization with 2-chloro-4,4,5,5-tetramethyl-1,3,2-dioxaphospholane (TMDP).

Table 2. Hydroxyl group relative content of the recovered lignin-enriched fraction determined by ^{31}P-NMR.

Functional group	Abbreviation	Chemical shift δ (ppm)	Relative content PT-EH^2 *Mxg*
Aliphatic OH	OH_{aliph}	145.5-150.0	0.9140 ± 0.0081
OH-Syringyl	OH_S	142.7-143.2	0.0055 ± 0.0002
OH-Guaicyl	OH_G	139,0-140.2	0.0290 ± 0.0049
OH-*p*-Hydroxyphenyl	OH_H	137.3-138.8	0.0285 ± 0.0015
OH-Carboxylic acid	OH_{COOH}	133.6-136.0	1.230 ± 0.0014

3.4. Insight into morphological observations of solid fractions

SEM micrograph of *Mxg* revealed the presence of compact and highly ordered fibers constituted by parallel stripes (**Figure 7.a**), as already reported (Auxenfans et al., 2017a, 2014). After [Emim][OAc]-pretreatment, the structural changes of *Mxg* are detected by the appearance of a smooth and more porous surface, which completely breaks down the initial microfibril network (**Figure 7.b**). The resulting pretreated material appeared more disorganized and expanded, with a larger surface area, which helps to explain the improved accessibility of hemicellulolytic enzymes to polymeric carbohydrates. The lignin-

enriched fractions (PT-EH *Mxg* and PT-EH^2 *Mxg*) showed an irregular morphology with sparse fibers and sheets in a poorly organized structure (**Figure 7.c** and **Figure 7.d**). In the literature, SEM micrographs of a solid fraction recovered after hydrothermal pretreatment and enzymatic hydrolysis of wheat straw showed rings and spirals attributed to secondary cell walls, which constitute vascular bundles with more lignified cell walls (Hansen et al., 2011). Based on this hypothesis, we suggested that the exposed fibers and sheets observed for the PT-EH *Mxg* and PT-EH^2 *Mxg* fractions may consist of the lignin polymer bound to residual polysaccharides.

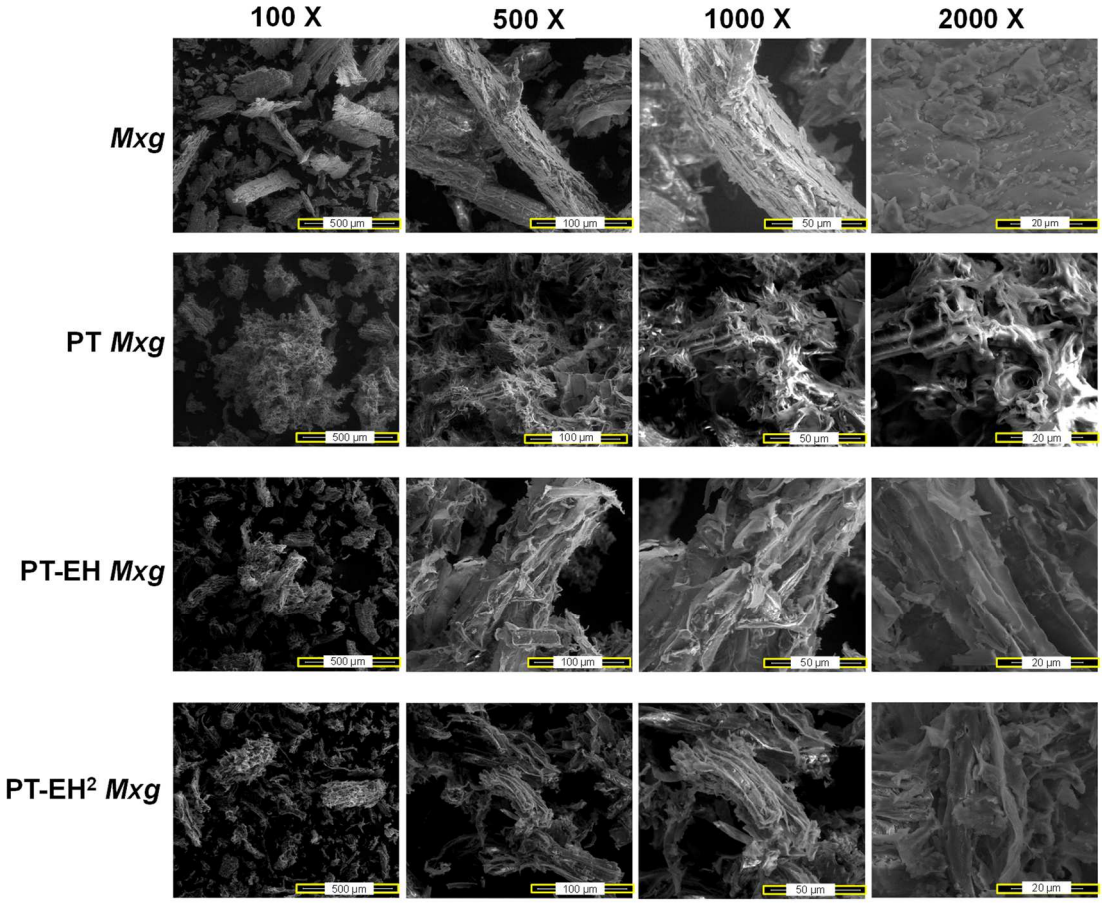

Figure 7. SEM micrographs of the recovered solid fractions after [Emim][OAc]-pretreatment and enzymatic hydrolyses of *Mxg.*

3.5. Mass balance of glucan, xylan and lignin

The fate of the main constituent polymers of *Mxg* and their respective masses in the different solid and liquid fractions throughout the sequential strategy is presented in **Figure 8**. The glucose mass balance evidenced a recovery of nearly 90% of D-glucose from *Mxg* in the liquid fractions while the remaining 10% was retained in the final solid fraction (PT-EH^2 *Mxg*), suggesting total recovery of D-glucose during the processing steps. Regarding the fate of D-xylose, the respective mass balance evidenced the recovery of 70% of D-xylose in hydrolysate and 10% in the final solid fraction. The remaining part (20%) was suggested to be solubilized in [Emim][OAc] highlighting a limited depolymerization of hemicelluloses during pretreatment. Finally, the sequential strategy allowed the isolation of 38% of the lignin polymer in the final solid fraction (PT-EH^2 *Mxg*), while 25% was solubilized in [Emim][OAc]. This global mass balance provided valuable data on the validity of this sequential strategy.

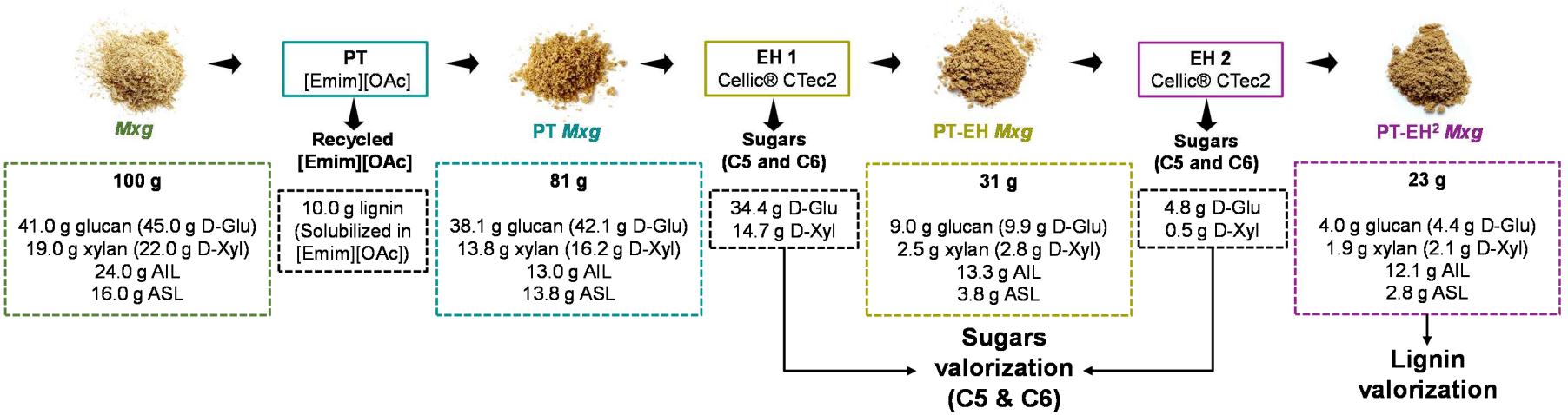

Figure 8. Global mass balance of polysaccharides and lignin after [Emim][OAc]-pretreatment and enzymatic hydrolyses of *Mxg*. *Mxg*= untreated *Miscanthus*, PT *Mxg*= pretreated *Miscanthus*. PT-EH *Mxg*= pretreated and hydrolyzed *Miscanthus*. PT-EH^2 *Mxg*= pretreated and double hydrolyzed *Miscanthus*, D-Glu= D-Glucose, D-Xyl= D-Xylose, AIL= acid insoluble lignin, ASL= acid soluble lignin.

3.6. Feasibility of enzymatic oxidative depolymerization of isolated lignin

Due to the high solubility of lignin in [Emim][OAc] (Figure A3. Supplementary data), the feasibility of LMS-catalyzed oxidative depolymerization of the lignin-enriched fraction in acetate buffer with [Emim][OAc] or recycled [Emim][OAc] as co-solvent, was studied. The [Emim][OAc] at 5% ($v.v^{-1}$) concentration was selected to ensure a compromise between substrate solubility and enzyme activity (Harwardt et al., 2014).

Regardless of the reaction medium, the LMS-catalyzed reaction led to the release of *p*-hydroxybenzaldehyde, as identified by HPLC. Similar concentrations were obtained in presence or absence of [Emim][OAc] (0.16 $mg.L^{-1}$ and 0.14 $mg.L^{-1}$ of *p*-hydroxybenzaldehyde, respectively) (**Figure 9.a**). Although the accessibility of the lignin-enriched substrate was expected to increase in the reactional medium supplemented with [Emim][OAc], no improvement in the reaction was observed, and the performance and selectivity of the LMS-catalyzed reaction did not seem to be affected. However, in presence of recycled [Emim][OAc], the amount of *p*-hydroxybenzaldehyde increased by a factor of 1.5, reaching a concentration of 0.23 ± 0.03 mg. L^{-1}. This higher concentration of *p*-hydroxybenzaldehyde highlighted the cumulative effects of (i) production by the LMS-catalyzed reaction (0.17 mg. L^{-1}) and (ii) previous solubilization in the ionic liquid [Emim][OAc] during pretreatment (0.06 mg. L^{-1} after dilution in aqueous buffer) (**Figure 9.a** and **Figure 9.b**). Although vanillic acid, syringic acid, vanillin, ferulic acid and *p*-coumaric acid were also quantified in recycled [Emim][OAc] (**Figure 9.b**), their absence in the media at

the end of the reaction suggested possible repolymerization reactions (Abdelaziz et al., 2016; Hilgers et al., 2018; Maijala et al., 2012). In the three reactive media, the production of *p*-hydroxybenzaldehyde from the lignin-enriched solid fraction (PT-EH^2 *Mxg*) by the LMS-catalyzed oxidative depolymerization reaction was demonstrated. The interest for this compound is related to its biological, antioxidant, flavoring, and antibacterial properties (Bountagkidou et al., 2010; Oh et al., 2017).

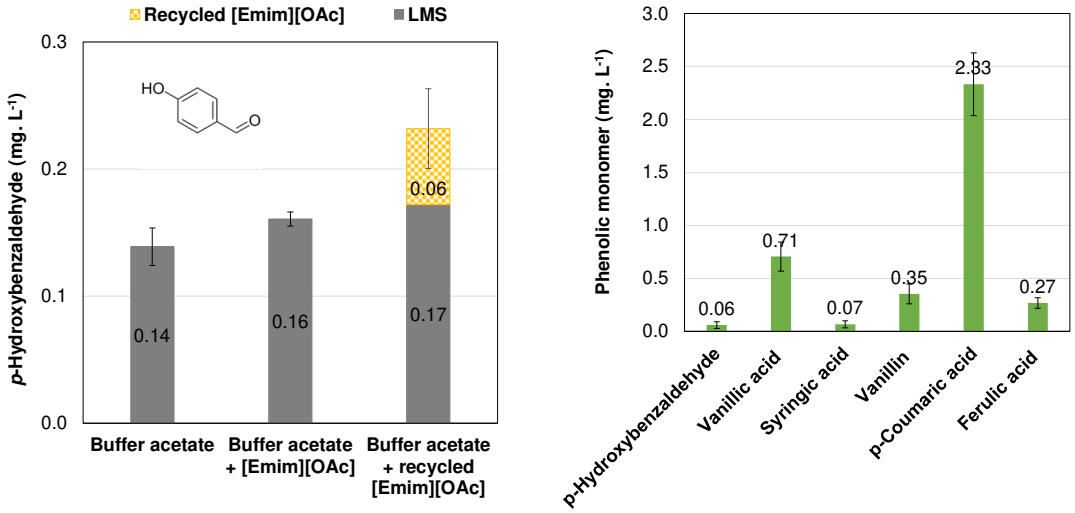

Figure 9. **(a)** Concentration of *p*-hydroxybenzaldehyde generated by the LMS-catalyzed oxidative depolymerization reaction in buffer acetate, buffer acetate + [Emim][OAc] and buffer acetate + recycled [Emim][OAc] after 24 h. **(b)** Phenolic monomers concentration in the initial reaction medium with recycled [Emim][OAc]. n=2. Average values ± standard deviation.

4. Conclusions

The pretreatment with the ionic liquid [Emim][OAc] and subsequent enzymatic transformations allowed the integrated co-valorization of cellulose, hemicelluloses and lignin polymers from *Miscanthus x giganteus*. Monomeric sugars (D-glucose and D-xylose) were produced with high hydrolysis performances. This study provides information on the fate of some valuable

phenolic compounds from the lignocellulosic matrix during the different processing steps. It was found that even steps not targeting the lignin polymer have an impact on the release of phenolic compounds. A lignin-enriched solid fraction was isolated, with a promising content superior to 50% $w.w^{-1}$. The performed structural and morphological studies evidenced the preserved structural integrity of lignin, similar to the so-called “native lignin”. The mass balance closure for lignin and polysaccharides validated the pertinence of the strategy. Finally, the feasibility of enzymatic oxidative depolymerization of the isolated lignin fraction for the production of phenolic intermediates such as *p*-hydroxybenzaldehyde was demonstrated.

Acknowledgements

Funding

The authors are grateful for the financial support from Hauts-de-France council to develop the STimule program -Enz4Lignin project. María Catalina QUESADA-SALAS is funded by the MESRI (*Ministère de l’Enseignement Supérieur de la Recherche et de l’Innovation).*

References

Abdelaziz, O.Y., Brink, D.P., Prothmann, J., Ravi, K., Sun, M., García-Hidalgo, J., Sandahl, M., Hulteberg, C.P., Turner, C., Lidén, G., Gorwa-Grauslund, M.F., 2016. Biological valorization of low molecular weight lignin. Biotechnol. Adv. 34, 1318–1346. https://doi.org/10.1016/j.biotechadv.2016.10.001

An, Y.X., Zong, M.H., Wu, H., Li, N., 2015. Pretreatment of lignocellulosic biomass with renewable cholinium ionic liquids: Biomass fractionation, enzymatic digestion and ionic liquid reuse. Bioresour. Technol. 192, 165–171. https://doi.org/10.1016/j.biortech.2015.05.064

Araya-Farias, M., Husson, E., Saavedra-Torrico, J., Gérard, D., Roulard, R., Gosselin, I., Rakotoarivonina, H., Lambertyn, V., Rémond, C., Sarazin, C., 2019. Wheat Bran Pretreatment by Room Temperature Ionic Liquid-Water Mixture: Optimization of Process Conditions by PLS-Surface Response Design. Front. Chem. 7, 1–15. https://doi.org/10.3389/fchem.2019.00585

Argyropoulos, D.S., 1995. 31P NMR In Wood Chemistry: A Review of Recent Progress. Res. Chem. Intermed. 21, 373–395. https://doi.org/10.1163/156856795X00314

Argyropoulos, D.S., 1994. Quantitative phosphorus-31 nmr analysis of lignins, a new tool for the lignin chemist. J. Wood Chem. Technol. 14, 45–63. https://doi.org/10.1080/02773819408003085

Argyropoulos, D.S., Pajer, N., Crestini, C., 2021. Quantitative ^{31}P NMR Analysis of Lignins and Tannins. J. Vis. Exp. 1–21. https://doi.org/10.3791/62696

Auxenfans, T., Buchoux, S., Husson, E., Sarazin, C., 2014. Efficient enzymatic saccharification of Miscanthus: Energy-saving by combining dilute acid and ionic liquid pretreatments. Biomass and Bioenergy 62, 82–92. https://doi.org/10.1016/j.biombioe.2014.01.011

Auxenfans, T., Crônier, D., Chabbert, B., Paës, G., 2017a. Understanding the structural and chemical changes of plant biomass following steam explosion pretreatment. Biotechnol. Biofuels 10, 1–16. https://doi.org/10.1186/s13068-017-0718-z

Auxenfans, T., Husson, E., Sarazin, C., 2017b. Simultaneous pretreatment and enzymatic saccharification of (ligno) celluloses in aqueous-ionic liquid media: A compromise. Biochem. Eng. J. 117, 77–86. https://doi.org/10.1016/j.bej.2016.10.004

Bajwa, D.S., Pourhashem, G., Ullah, A.H., Bajwa, S.G., 2019. A concise review of current lignin production, applications, products and their environment impact. Ind. Crops Prod. 139, 111526. https://doi.org/10.1016/j.indcrop.2019.111526

Baruah, J., Nath, B.K., Sharma, R., Kumar, S., Deka, R.C., Baruah, D.C., Kalita, E., 2018. Recent trends in the pretreatment of lignocellulosic biomass for value-added products. Front. Energy Res. 6, 1–19. https://doi.org/10.3389/fenrg.2018.00141

Beckham, G.T., Johnson, C.W., Karp, E.M., Salvachúa, D., Vardon, D.R., 2016. Opportunities and challenges in biological lignin valorization. Curr. Opin. Biotechnol. 42, 40–53. https://doi.org/10.1016/j.copbio.2016.02.030

Bertella, S., Luterbacher, J.S., 2020. Lignin Functionalization for the Production

609 of Novel Materials. Trends Chem. 2, 440–453.
610 https://doi.org/10.1016/j.trechm.2020.03.001
611 Bhatia, R., Lad, J.B., Bosch, M., Bryant, D.N., Leak, D., Hallett, J.P., Franco,
612 T.T., Gallagher, J.A., 2021. Production of oligosaccharides and biofuels
613 from Miscanthus using combinatorial steam explosion and ionic liquid
614 pretreatment. Bioresour. Technol. 323, 124625.
615 https://doi.org/10.1016/j.biortech.2020.124625
616 Bhatia, R., Winters, A., Bryant, D.N., Bosch, M., Clifton-Brown, J., Leak, D.,
617 Gallagher, J., 2020. Pilot-scale production of xylo-oligosaccharides and
618 fermentable sugars from Miscanthus using steam explosion pretreatment.
619 Bioresour. Technol. 296. https://doi.org/10.1016/j.biortech.2019.122285
620 Bhatia, S.K., Jagtap, S.S., Bedekar, A.A., Bhatia, R.K., Patel, A.K., Pant, D.,
621 Rajesh Banu, J., Rao, C. V., Kim, Y.G., Yang, Y.H., 2020. Recent
622 developments in pretreatment technologies on lignocellulosic biomass:
623 Effect of key parameters, technological improvements, and challenges.
624 Bioresour. Technol. 300, 122724.
625 https://doi.org/10.1016/j.biortech.2019.122724
626 Bountagkidou, O.G., Ordoudi, S.A., Tsimidou, M.Z., 2010. Structure-antioxidant
627 activity relationship study of natural hydroxybenzaldehydes using in vitro
628 assays. Food Res. Int. 43, 2014–2019.
629 https://doi.org/10.1016/j.foodres.2010.05.021
630 Brandt-Talbot, A., Gschwend, F.J.V., Fennell, P.S., Lammens, T.M., Tan, B.,
631 Weale, J., Hallett, J.P., 2017. An economically viable ionic liquid for the
632 fractionation of lignocellulosic biomass. Green Chem. 19, 3078–3102.
633 https://doi.org/10.1039/c7gc00705a
634 Brosse, N., Dufour, A., Meng, X., Sun, Q., Ragauskas, A., 2012. Miscanthus: a
635 fast- growing crop for biofuels and chemicals production. Biofuels, Bioprod.
636 Biorefining 6, 246–256. https://doi.org/10.1002/bbb
637 Browning, B.L., 1967. Methods of Wood Chemistry, Volumes I & II. John Wiley
638 & Sons, New York, USA.
639 Crestini, C., Argyropoulos, D.S., 1997. Structural Analysis of Wheat Straw
640 Lignin by Quantitative 31P and 2D NMR Spectroscopy. The Occurrence of
641 Ester Bonds and α-O-4 Substructures. J. Agric. Food Chem. 45, 1212–
642 1219. https://doi.org/10.1021/jf960568k
643 Deuss, P.J., Kugge, C., 2021. “Lignin-first” catalytic valorization for generating
644 higher value from lignin. Chem Catal. 1, 8–11.
645 https://doi.org/10.1016/j.checat.2021.05.004
646 Dillies, J., Vivien, C., Chevalier, M., Rulence, A., Châtaigné, G., Flahaut, C.,
647 Senez, V., Froidevaux, R., 2020. Enzymatic depolymerization of industrial
648 lignins by laccase-mediator systems in 1,4-dioxane/water. Biotechnol. Appl.
649 Biochem. 67, 774–782. https://doi.org/10.1002/bab.1887
650 Elgharbawy, A.A., Alam, M.Z., Moniruzzaman, M., Goto, M., 2016. Ionic liquid
651 pretreatment as emerging approaches for enhanced enzymatic hydrolysis
652 of lignocellulosic biomass. Biochem. Eng. J. 109, 252–267.
653 https://doi.org/10.1016/j.bej.2016.01.021
654 Fi, I.F., Peter, F., Boeriu, C.G., 2013. Structural Analysis of Lignins from
655 Different Sources. World Acad. Sci. Enginnering Technol. 7, 98–103.
656 Goshadrou, A., Lefsrud, M., 2017. Synergistic surfactant-assisted [EMIM]OAc

657 pretreatment of lignocellulosic waste for enhanced cellulose accessibility to
658 cellulase. Carbohydr. Polym. 166, 104–113.
659 https://doi.org/10.1016/j.carbpol.2017.02.076
660 Guo, Z., Li, D., You, T., Zhang, Xun, Xu, F., Zhang, Xueming, Yang, Y., 2020.
661 New Lignin Streams Derived from Heteropoly Acids Enhanced Neutral
662 Deep Eutectic Solvent Fractionation: Toward Structural Elucidation and
663 Antioxidant Performance. ACS Sustain. Chem. Eng. 8, 12110–12119.
664 https://doi.org/10.1021/acssuschemeng.0c03491
665 Hage, R. El, Brosse, N., Chrusciel, L., Sanchez, C., Sannigrahi, P., Ragauskas,
666 A., 2009. Characterization of milled wood lignin and ethanol organosolv
667 lignin from miscanthus. Polym. Degrad. Stab. 94, 1632–1638.
668 https://doi.org/10.1016/j.polymdegradstab.2009.07.007
669 Hansen, M.A.T., Kristensen, J.B., Felby, C., Jørgensen, H., 2011. Pretreatment
670 and enzymatic hydrolysis of wheat straw (Triticum aestivum L.) - The
671 impact of lignin relocation and plant tissues on enzymatic accessibility.
672 Bioresour. Technol. 102, 2804–2811.
673 https://doi.org/10.1016/j.biortech.2010.10.030
674 Harwardt, N., Stripling, N., Roth, S., Liu, H., Schwaneberg, U., Spiess, A.C.,
675 2014. Effects of ionic liquids on the reaction kinetics of a laccase-mediator
676 system. RSC Adv. 4, 17097–17104. https://doi.org/10.1039/c4ra00733f
677 Hilgers, R., Vincken, J.P., Gruppen, H., Kabel, M.A., 2018. Laccase/Mediator
678 Systems: Their Reactivity toward Phenolic Lignin Structures. ACS Sustain.
679 Chem. Eng. 6, 2037–2046.
680 https://doi.org/10.1021/acssuschemeng.7b03451
681 Horikawa, Y., Hirano, S., Mihashi, A., Kobayashi, Y., Zhai, S., Sugiyama, J.,
682 2019. Prediction of Lignin Contents from Infrared Spectroscopy: Chemical
683 Digestion and Lignin/Biomass Ratios of Cryptomeria japonica. Appl.
684 Biochem. Biotechnol. 188, 1066–1076. https://doi.org/10.1007/s12010-019-
685 02965-8
686 Hulin, L., Husson, E., Bonnet, J.P., Stevanovic, T., Sarazin, C., 2015.
687 Enzymatic Transesterification of Kraft Lignin with long Acyl Chains in Ionic
688 Liquids. Molecules 20, 16334–16353.
689 https://doi.org/10.3390/molecules200916334
690 Husson, E., Auxenfans, T., Herbaut, M., Baralle, M., Lambertyn, V.,
691 Rakotoarivonina, H., Rémond, C., Sarazin, C., 2018. Sequential and
692 simultaneous strategies for biorefining of wheat straw using room
693 temperature ionic liquids, xylanases and cellulases. Bioresour. Technol.
694 251, 280–287. https://doi.org/10.1016/j.biortech.2017.12.047
695 Husson, E., Hulin, L., Hadad, C., Boughanmi, C., Stevanovic, T., Sarazin, C.,
696 2019. Acidic Ionic Liquid as Both Solvent and Catalyst for Fast Chemical
697 Esterification of Industrial Lignins: Performances and Regioselectivity.
698 Front. Chem. 7, 1–13. https://doi.org/10.3389/fchem.2019.00578
699 Imman, S., Khongchamnan, P., Wanmolee, W., Laosiripojana, N., Kreetachat,
700 T., Sakulthaew, C., Chokejaroenrat, C., Suriyachai, N., 2021. Fractionation
701 and characterization of lignin from sugarcane bagasse using a sulfuric acid
702 catalyzed solvothermal process. RSC Adv. 11, 26773–26784.
703 https://doi.org/10.1039/d1ra03237b
704 Jung, W., Savithri, D., Sharma-Shivappa, R., Kolar, P., 2020. Effect of Sodium

Hydroxide Pretreatment on Lignin Monomeric Components of Miscanthus × giganteus and Enzymatic Hydrolysis. Waste and Biomass Valorization 11, 5891–5900. https://doi.org/10.1007/s12649-019-00859-8
Kim, G.H., Um, B.H., 2020. Fractionation and characterization of lignins from Miscanthus via organosolv and soda pulping for biorefinery applications. Int. J. Biol. Macromol. 158, 443–451. https://doi.org/10.1016/j.ijbiomac.2020.04.229
Kim, S.J., Kim, M.Y., Jeong, S.J., Jang, M.S., Chung, I.M., 2012. Analysis of the biomass content of various Miscanthus genotypes for biofuel production in Korea. Ind. Crops Prod. 38, 46–49. https://doi.org/10.1016/j.indcrop.2012.01.003
Klemm, D., Heublein, B., Fink, H.P., Bohn, A., 2005. Cellulose: Fascinating biopolymer and sustainable raw material. Angew. Chemie - Int. Ed. 44, 3358–3393. https://doi.org/10.1002/anie.200460587
Laurichesse, S., Avérous, L., 2014. Chemical modification of lignins: Towards biobased polymers. Prog. Polym. Sci. 39, 1266–1290. https://doi.org/10.1016/j.progpolymsci.2013.11.004
Le Ngoc Huyen, T., Rémond, C., Dheilly, R.M., Chabbert, B., 2010. Effect of harvesting date on the composition and saccharification of Miscanthus x giganteus. Bioresour. Technol. 101, 8224–8231. https://doi.org/10.1016/j.biortech.2010.05.087
Lee, E.A., Kim, J.K., Bandi, R., Dadigala, R., Han, S.Y., Kwon, G.J., Gwon, J., Youe, W.J., Park, J.S., Park, C.W., Kim, N.H., Lee, S.H., 2022. Ionic Liquid-assisted Isolation of Lignin From Lignocellulose and Its Esterification with Fatty Acids. BioResources 17, 5861–5877. https://doi.org/10.15376/biores.17.4.5861-5877
Lopes, J.M., Bermejo, M.D., Martín, Á., Cocero, M.J., 2017. Ionic liquid as reaction media for the production of cellulose-derived polymers from cellulosic biomass. ChemEngineering 1, 1–28. https://doi.org/10.3390/chemengineering1020010
Maijala, P., Mattinen, M.L., Nousiainen, P., Kontro, J., Asikkala, J., Sipilä, J., Viikari, L., 2012. Action of fungal laccases on lignin model compounds in organic solvents. J. Mol. Catal. B Enzym. 76, 59–67. https://doi.org/10.1016/j.molcatb.2011.12.009
Moreno, A.D., Tomás-Pejó, E., Ballesteros, M., Negro, M.J., 2019. Pretreatment technologies for lignocellulosic biomass deconstruction within a biorefinery perspective. Biomass, Biofuels, Biochem. Biofuels Altern. Feed. Convers. Process. Prod. Liq. Gaseous Biofuels 379–399. https://doi.org/10.1016/B978-0-12-816856-1.00016-6
Narron, R.H., Kim, H., Chang, H.M., Jameel, H., Park, S., 2016. Biomass pretreatments capable of enabling lignin valorization in a biorefinery process. Curr. Opin. Biotechnol. 38, 39–46. https://doi.org/10.1016/j.copbio.2015.12.018
Ninomiya, K., Ochiai, K., Eguchi, M., Kuroda, K., Tsuge, Y., Ogino, C., Taima, T., Takahashi, K., 2018. Oxidative depolymerization potential of biorefinery lignin obtained by ionic liquid pretreatment and subsequent enzymatic saccharification of eucalyptus. Ind. Crops Prod. 111, 457–461. https://doi.org/10.1016/j.indcrop.2017.10.056

Oh, S.H., Ryu, B.M., Ngo, D.H., Kim, W.S., Kim, D.G., Kim, S.K., 2017. 4-hydroxybenzaldehyde-chitooligomers suppresses H2O2-induced oxidative damage in microglia BV-2 cells. Carbohydr. Res. 440–441, 32–37. https://doi.org/10.1016/j.carres.2017.01.007

Ostadjoo, S., Berton, P., Shamshina, J.L., Rogers, R.D., 2018. Scaling-up ionic liquid-based technologies: How much do we care about their toxicity? Prima facie information on 1-ethyl-3-methylimidazolium acetate. Toxicol. Sci. 161, 249–265. https://doi.org/10.1093/toxsci/kfx172

Ovejero-Pérez, A., Rigual, V., Domínguez, J.C., Alonso, M.V., Oliet, M., Rodriguez, F., 2020. Acidic depolymerization vs ionic liquid solubilization in lignin extraction from eucalyptus wood using the protic ionic liquid 1-methylimidazolium chloride. Int. J. Biol. Macromol. 157, 461–469. https://doi.org/10.1016/j.ijbiomac.2020.04.194

Patil, V., Adhikari, S., Cross, P., Jahromi, H., 2020. Progress in the solvent depolymerization of lignin. Renew. Sustain. Energy Rev. 133, 110359. https://doi.org/10.1016/j.rser.2020.110359

Rezania, S., Oryani, B., Cho, J., Talaiekhozani, A., Sabbagh, F., Hashemi, B., Rupani, P.F., Mohammadi, A.A., 2020. Different pretreatment technologies of lignocellulosic biomass for bioethanol production: An overview. Energy 199, 117457. https://doi.org/10.1016/j.energy.2020.117457

Sathitsuksanoh, N., Holtman, K.M., Yelle, D.J., Morgan, T., Stavila, V., Pelton, J., Blanch, H., Simmons, B.A., George, A., 2014. Lignin fate and characterization during ionic liquid biomass pretreatment for renewable chemicals and fuels production. Green Chem. 16, 1236–1247. https://doi.org/10.1039/c3gc42295j

Sethupathy, S., Murillo Morales, G., Gao, L., Wang, H., Yang, B., Jiang, J., Sun, J., Zhu, D., 2022. Lignin valorization: Status, challenges and opportunities. Bioresour. Technol. 347, 126696. https://doi.org/10.1016/j.biortech.2022.126696

Singh Arora, D., Kumar Sharma, R., 2010. Ligninolytic fungal laccases and their biotechnological applications. Appl. Biochem. Biotechnol. 160, 1760–1788. https://doi.org/10.1007/s12010-009-8676-y

Sluiter, A., Hames, B., Ruiz, R., Scarlata, C., Sluiter, J., Templeton, D., 2005a. Determination of Ash in Biomass. Laboratory Analytical Procedure NREL/TP-510-42622. National Renewable Energy Laboratory (NREL). Colorado, USA.

Sluiter, A., Hames, B., Ruiz, R., Scarlata, C., Sluiter, J., Templeton, D., Crocker, D., 2012. Determination of Structural Carbohydrates and Lignin in Biomass. Laboratory Analytical Procedure NREL/TP-510-42618. Renewable Energy Laboratory (NREL), National Renewable Energy Laboratory (NREL). Colorado, USA.

Sluiter, A., Ruiz, R., Scarlata, C., Sluiter, J., Templeton, D., 2005b. Determination of Extractives in Biomass. Laboratory Analytical Procedure (LAP). National Renewable Energy Laboratory (NREL). NREL/TP-510-42619. Colorado, USA.

Smuga-Kogut, M., Szymanowska-Powałowska, D., Markiewicz, R., Piskier, T., Kogut, T., 2021. Ionic liquid pretreatment of stinging nettle stems and giant miscanthus for bioethanol production. Sci. Rep. 11, 1–11.

https://doi.org/10.1038/s41598-021-97993-y
Sun, Y., Xue, B., 2018. Understanding structural changes in the lignin of Eucalyptus urophylla during pretreatment with an ionic liquid-water mixture. Ind. Crops Prod. 123, 600–609. https://doi.org/10.1016/j.indcrop.2018.07.029
Sun, Z., Fridrich, B., De Santi, A., Elangovan, S., Barta, K., 2018. Bright Side of Lignin Depolymerization: Toward New Platform Chemicals. Chem. Rev. 118, 614–678. https://doi.org/10.1021/acs.chemrev.7b00588
Talebi Amiri, M., Dick, G.R., Questell-Santiago, Y.M., Luterbacher, J.S., 2019. Fractionation of lignocellulosic biomass to produce uncondensed aldehyde-stabilized lignin. Nat. Protoc. 14, 921–954. https://doi.org/10.1038/s41596-018-0121-7
Tarasov, D., Leitch, M., Fatehi, P., 2018. Lignin-carbohydrate complexes: Properties, applications, analyses, and methods of extraction: A review. Biotechnol. Biofuels 11, 1–28. https://doi.org/10.1186/s13068-018-1262-1
Tian, D., Hu, J., Chandra, R.P., Saddler, J.N., Lu, C., 2017. Valorizing Recalcitrant Cellulolytic Enzyme Lignin via Lignin Nanoparticles Fabrication in an Integrated Biorefinery. ACS Sustain. Chem. Eng. 5, 2702–2710. https://doi.org/10.1021/acssuschemeng.6b03043
Usmani, Z., Sharma, M., Gupta, P., Karpichev, Y., Gathergood, N., Bhat, R., Gupta, V.K., 2020. Ionic liquid based pretreatment of lignocellulosic biomass for enhanced bioconversion. Bioresour. Technol. 304, 123003. https://doi.org/10.1016/j.biortech.2020.123003
Villaverde, J.J., Li, J., Ek, M., Ligero, P., De Vega, A., 2009. Native lignin structure of Miscanthus x giganteus and its changes during acetic and formic acid fractionation. J. Agric. Food Chem. 57, 6262–6270. https://doi.org/10.1021/jf900483t
Wang, H., Chen, W., Zhang, X., Wei, Y., Zhang, A., Liu, S., Wang, X., Liu, C., 2018. Structural changes of bagasse dusring the homogeneous esterification with maleic anhydride in ionic liquid 1-Allyl-3-methylimidazolium chloride. Polymers (Basel). 10, 1–8. https://doi.org/10.3390/polym10040433
Wang, H., Pu, Y., Ragauskas, A., Yang, B., 2019. From lignin to valuable products–strategies, challenges, and prospects. Bioresour. Technol. 271, 449–461. https://doi.org/10.1016/j.biortech.2018.09.072
Wang, K., Bauer, S., Sun, R.C., 2012. Structural transformation of miscanthus ×giganteus lignin fractionated under mild formosolv, basic organosolv, and cellulolytic enzyme conditions. J. Agric. Food Chem. 60, 144–152. https://doi.org/10.1021/jf2037399
Yoo, C.G., Pu, Y., Ragauskas, A.J., 2017. Ionic liquids: Promising green solvents for lignocellulosic biomass utilization. Curr. Opin. Green Sustain. Chem. 5, 5–11. https://doi.org/10.1016/j.cogsc.2017.03.003
Yoon, L.W., Ang, T.N., Ngoh, G.C., Chua, A.S.M., 2012. Regression analysis on ionic liquid pretreatment of sugarcane bagasse and assessment of structural changes. Biomass and Bioenergy 36, 160–169. https://doi.org/10.1016/j.biombioe.2011.10.033
Yu, O., Kim, K.H., 2020. Lignin to materials: A focused review on recent novel lignin applications. Appl. Sci. 10. https://doi.org/10.3390/app10134626

Yuan, T.Q., Sun, S.N., Xu, F., Sun, R.C., 2011. Characterization of lignin structures and lignin-carbohydrate complex (LCC) linkages by quantitative 13C and 2D HSQC NMR spectroscopy. J. Agric. Food Chem. 59, 10604–10614. https://doi.org/10.1021/jf2031549

Zevallos Torres, L.A., Lorenci Woiciechowski, A., de Andrade Tanobe, V.O., Karp, S.G., Guimarães Lorenci, L.C., Faulds, C., Soccol, C.R., 2020. Lignin as a potential source of high-added value compounds: A review. J. Clean. Prod. 263. https://doi.org/10.1016/j.jclepro.2020.121499

Zhang, Q., Hu, J., Lee, D.J., 2017. Pretreatment of biomass using ionic liquids: Research updates. Renew. Energy 111, 77–84. https://doi.org/10.1016/j.renene.2017.03.093

Zhang, Y., Naebe, M., 2021. Lignin: A Review on Structure, Properties, and Applications as a Light-Colored UV Absorber. ACS Sustain. Chem. Eng. 9, 1427–1442. https://doi.org/10.1021/acssuschemeng.0c06998

Zhao, W., Xiao, L.P., Song, G., Sun, R.C., He, L., Singh, S., Simmons, B.A., Cheng, G., 2017. From lignin subunits to aggregates: Insights into lignin solubilization. Green Chem. 19, 3272–3281. https://doi.org/10.1039/c7gc00944e